International Journal of Pressure Vessels and Piping 168 (2018) 94–99

Contents lists available at ScienceDirect

International Journal of Pressure Vessels and Piping

journal homepage: www.elsevier.com/locate/ijpvp

Influence of ovalisation on the plastic collapse of thick cylindrical tubes under uniform bending

Jie Wang[1], Adam J. Sadowski[*,2], J.Michael Rotter[3]

Department of Civil and Environmental Engineering, Imperial College London, United Kingdom

ARTICLE INFO

Keywords:
Thick tube
Cylindrical shell
Plastic collapse
Ovalisation
Plane strain
Length effect

ABSTRACT

An accurate assessment of the bending resistance of thick cylindrical metal tubes is necessary for the safe and efficient design of pipelines, piles, pressure vessels, circular hollow sections and other common tubular structures. Bending tests continue to be widely performed as part of many engineering research programmes, but despite their ubiquity they often generate results that are difficult to interpret. Discrepancies from the attainment of the classical full plastic moment are common and often attributed to a mixture of ovalisation, local buckling, imperfections and strain hardening. However, the effects of these phenomena are yet to be quantified in isolation, even for a system as classical as a cylinder under uniform bending.

The goal of this computational study is to quantify the extent to which geometrically nonlinear effects, specifically ovalisation and bifurcation buckling, may depress the resistance of a thick perfect cylinder under uniform bending that would otherwise be expected to attain the full plastic moment. Simulations are performed using two- and three-dimensional finite element models with a simple ideal elastic-plastic material law that excludes the influence of strain hardening. The study aims to arm designers of test programmes on the bending of tubulars with 'rules of thumb' to approximately quantify the likely influence of tube length on their results, recently shown to be an important parameter controlling geometric nonlinearity. For thick tubes, ovalisation at the plastic limit state under bending is found to be almost negligible.

1. Introduction

Research into the response of tubulars under bending continues to be widely conducted despite the apparent simplicity of the cylindrical geometry and the apparent ease with which this allows a first estimate of the elastic buckling and plastic collapse resistances. A significant database of test results has been accumulated over several decades, supported by an increasingly rich body of research based on theoretical and computational studies. An illustration of 141 test results for tubes under bending gathered from the literature is shown in Fig. 1, where the measured dimensionless characteristic resistance M_k/M_{pl} of each tube is plotted against its dimensionless length $\Omega = (L/r)\sqrt{(t/r)}$ and dimensionless cross-sectional slenderness $d/(t\varepsilon^2)$. Here L, r and t are the cylinder length, mid-surface radius and thickness respectively, and σ_y is the yield stress such that $\varepsilon^2 = 235/\sigma_y$. The full plastic moment M_{pl} is given by:

$$M_{pl} = \frac{4}{3}\sigma_y\left[\left(r+\frac{t}{2}\right)^3 - \left(r-\frac{t}{2}\right)^3\right] \quad (1)$$

The measured values of the control test 0.2% proof stress σ_y were used in constructing the illustration in Fig. 1, but only nominal values for the geometry since measured values are usually not available. The data is taken from publications from research programmes on carbon steel tubes under four-point bending tests both historical [1–3] and recent (RFCS Combitube [4] and follow-up tests in Rotterdam [5]). The reader is invited to consult the reference list of Buchanan *et al.* [6] for the sources of the studies shown in Fig. 1 but not referenced here for brevity.

The parameter Ω has a long history, being closely related to the well-known Batdorf parameter $Z = L^2/(rt)\sqrt{(1-\nu^2)}$ [7] (where ν is the Poisson ratio), but the current notation was coined by Calladine [8]. It was later confirmed by Rotter *et al.* [9] that Ω is the relevant dimensionless group that controls pre-buckling ovalisation in cylinders

* Corresponding author.
E-mail address: a.sadowski@imperial.ac.uk (A.J. Sadowski).
[1] Post-Doctoral Researcher in Structural Engineering.
[2] Lecturer in Structural Engineering.
[3] Visiting Emeritus Professor of Civil Engineering.

https://doi.org/10.1016/j.ijpvp.2018.05.004
Received 16 February 2018; Accepted 5 May 2018
Available online 08 May 2018

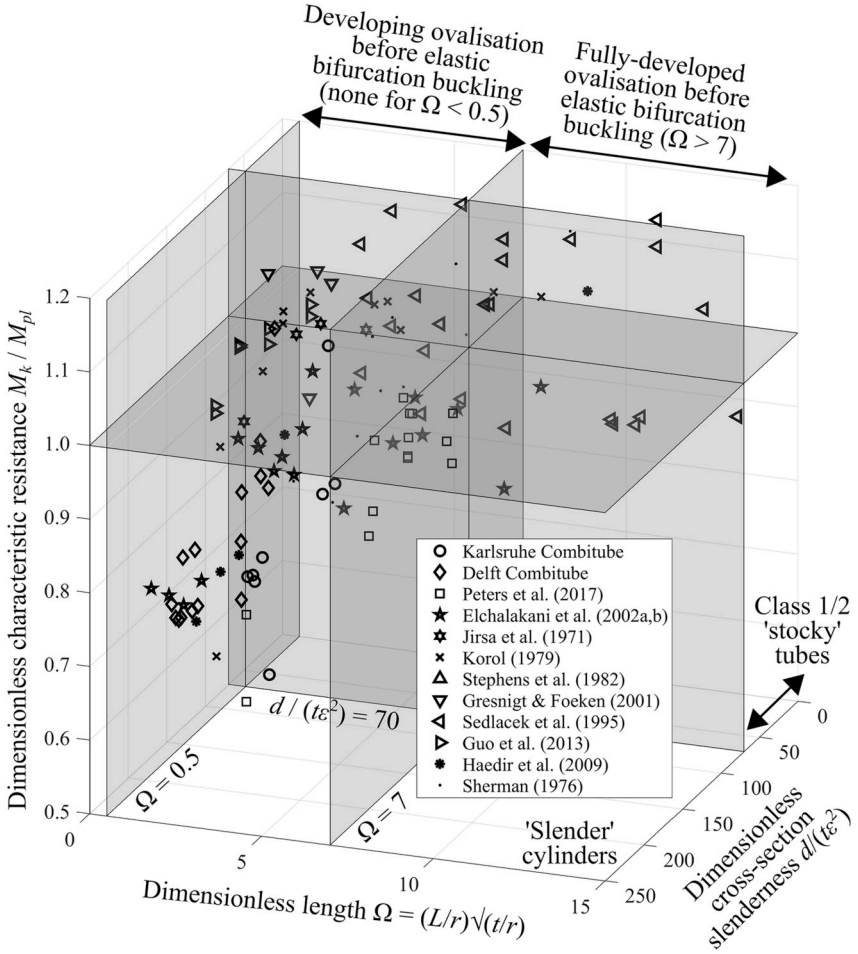

Fig. 1. Three-dimensional presentation of 141 tests on cylinders under bending. The dimensionless characteristic resistance M_k/M_{pl} is plotted against the dimensionless length $\Omega = (L/r)\sqrt{(t/r)}$ and dimensionless cross-section slenderness $d/(t\varepsilon^2)$, assuming a measured yield stress but nominal geometry.

under uniform bending. Ovalisation was found to be entirely absent from the elastic response of cylinders shorter than $\Omega = 0.5$ but plays an increasingly important role for cylinders longer than this, becoming fully-developed (invariant with further increases in length) beyond $\Omega \approx 7$ where it causes a reduction in the bifurcation buckling moment of close to 50% under elastic conditions. It should be stressed that ovalisation occurs on the fundamental equilibrium path and precedes the inelastic response. While its effect on the elastic buckling capacity of thin cylinders is now well understood [9–11], its influence on the plastic limit moment in a thick tube is significantly less so.

It may be seen in Fig. 1 that virtually all tests exhibit $\Omega > 0.5$. Consequently, it is to be expected that their fundamental response may be, to a greater or lesser extent, affected by geometrically nonlinear effects such as ovalisation. Yet despite this, a significant portion of tests of 'stocky' tubes with $d/(t\varepsilon^2) < \sim 70$ (approximately the internationally-accepted upper slenderness limit for 'Class 1 or 2' sections; see Table 13 in Gresnigt and Karamanos [12] attain and exceed the full plastic moment even for $\Omega > > 7$). This suggests that ovalisation is likely to only have a negligible effect on the plastic limit moment of thick tubes. This hypothesis is explored computationally in this study.

2. Modelling with finite elements

2.1. Scope of the study

This study seeks to quantify computationally the probable influence of ovalisation on the moment capacity of unpressurised thick cylindrical tubes under uniform bending when dominated by plasticity. A comprehensive set of finite element analyses was performed using the ABAQUS software [13] to investigate the following:

- Cylinders with a range of lengths between those that are short enough to be unaffected by ovalisation but long enough to be free of boundary restraint effects ($5r/t < \Omega < 0.5$) to those long enough to experience fully-developed ovalisation before elastic bifurcation buckling ($\Omega > 7$).
- Cylinders with relative slendernesses ranging from very stocky ($d/(t\varepsilon^2) < 70$) to quite slender ($d/(t\varepsilon^2) > 500$), studied for three generic yield stresses σ_y = 235, 355 and 460 MPa and varying d/t ratios.

Two sources of great ambiguity, the influences of imperfections and strain hardening, were purposefully omitted to allow the influence of geometrical nonlinearity to be studied in isolation. For each combination of parameters, the following computational analyses were performed [14]:

- Materially nonlinear but geometrically linear analysis (MNA) to obtain the classical plastic limit moment of the perfect tube.
- Geometrically nonlinear but materially linear analysis (GNA) to obtain the nonlinear elastic bifurcation buckling resistance of the perfect tube.
- Geometrically and materially nonlinear analysis (GMNA) to obtain the characteristic nonlinear elastic-plastic resistance of the perfect tube.

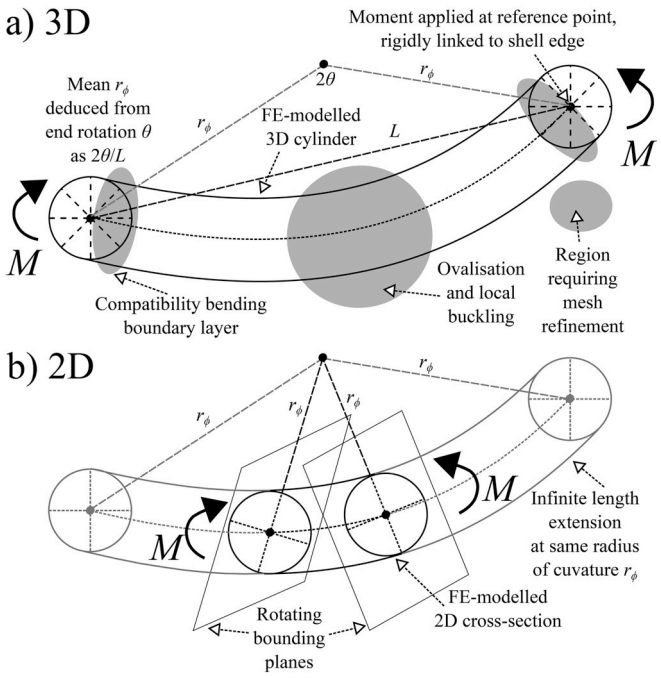

Fig. 2. Schematic illustrating the a) 3D and b) 2D systems modelled with FE, where r_ϕ is the (mean) longitudinal radius of curvature.

Three-dimensional models using 3D shell finite elements were employed, but an additional set of analyses was performed using a 2D generalised plane strain formulation to investigate the asymptotic behaviour of 'infinitely' long tubes. In all cases, an elastic modulus of $E = 200$ GPa and Poisson ratio of $\nu = 0.3$ were assumed.

2.2. Conventional 3D shell model

A previous study by the authors [15] showed that shear-flexible 3D shell elements such as the reduced-integration linear S4R element are capable of accurately predicting the response of tubes as thick as $d/t = 20$ ($r/t = 10$) under uniform bending efficiently, with thick shell elements both predicting the same response as solid-continuum elements and reproducing test results with high fidelity at only a fraction of the computational cost. Consequently, the S4R element was used in all 3D models in this study, with details of load application and boundary conditions illustrated in the schematic in Fig. 2a. In the interest of brevity, the reader may consult the authors' previous publications for modelling details [9,15,16] as these employed the same arrangement and meshing schemes.

2.3. Generalised 2D plane strain model

It is known that a long elastic perfect cylinder under uniform bending will fail by local bifurcation buckling on the flattened compressed side at a moment approximately 5% below the Brazier elastic limit moment M_{Braz} (Eq. (2); [9,11,16]), and far below the elastic critical bifurcation buckling moment M_{cr} (Eq. (3)). This reduction is due to an increased local circumferential radius of curvature reducing both the critical buckling stress and the lever arm at the most ovalised cross-section. Both ovalisation and local bifurcation buckling thus inevitably afflict a buckling prediction from a 3D analysis. By contrast, a 2D generalised plane strain model allows the direct simulation of the cross-section of an infinitely-long tube by enforcing a constant longitudinal curvature and thus truly uniform bending (Fig. 2b), with only limit point snap-through buckling possible under a loss of cross-sectional stability. This allows an accurate evaluation of the asymptotic behaviour as $\Omega \to \infty$, that is unachievable with 3D models. The 4-node bilinear quadrilateral reduced-integration CPEG4R element was used here, with at least 4 elements through the thickness.

$$M_{Braz} = \frac{2\pi\sqrt{2}}{9}\frac{Ert^2}{\sqrt{1-\nu^2}} \approx 0.99\frac{Ert^2}{\sqrt{1-\nu^2}} \tag{2}$$

$$M_{cr} \approx 1.81\frac{Ert^2}{\sqrt{1-\nu^2}} \approx 1.83M_{Braz} \tag{3}$$

2.4. Comparison between 3D and 2D finite element models and reference theory

A brief illustration of the validity of the predictions for a tube with $d/t = 200$ ($r/t = 100$) by the above two modelling approaches is presented in Fig. 3. Here, 2D GNA predictions of the nonlinear elastic moment-curvature relationships (made dimensionless using Eqs (3) and

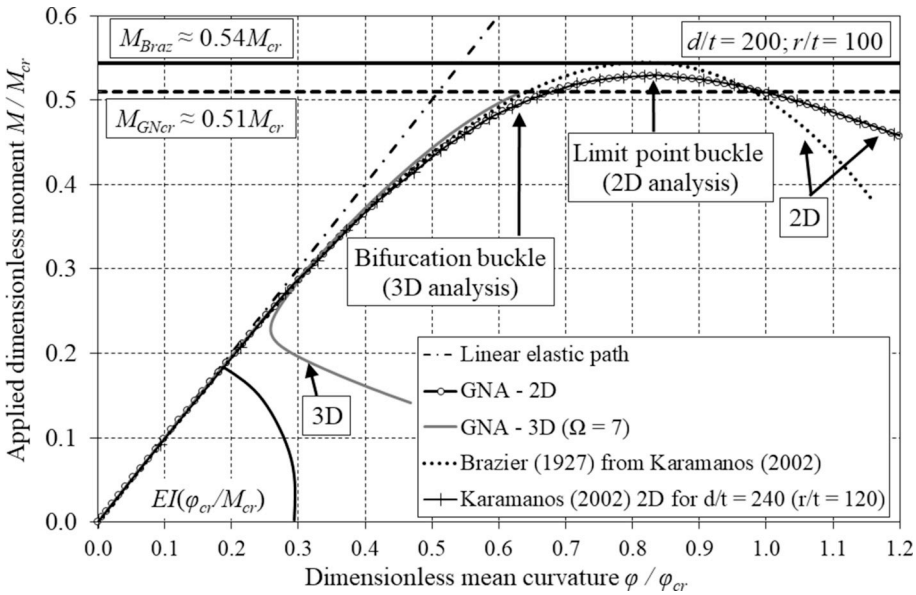

Fig. 3. Comparison of nonlinear elastic moment-curvature equilibrium paths obtained from the 2D and 3D GNA models and the predictions in Karamanos [11] for the elastic buckling of 'long' cylinders under uniform bending.

(4), where φ_{cr} is the mean longitudinal curvature at buckling as predicted by linear bending theory) are compared with 3D GNA predictions for a perfect cylinder at $\Omega = 7$. Both GNAs are additionally compared with the algebraic moment-curvature relationship of Brazier [10] as reported in Table 1 of Karamanos [11]; as well as the predictions of that author's own 2D FE formulation for $d/t = 240$ ($r/t = 120$; digitised from Fig. 7 of that paper). For the 3D analysis, the longitudinal curvature should be understood in an averaged sense over the length of the cylinder (Fig. 2a).

$$\varphi_{cr} \approx \frac{t}{r^2\sqrt{3(1-\nu^2)}} \tag{4}$$

It is shown that a 2D generalised plane strain model accurately reproduces the Brazier relationship and undergoes limit point buckling at a moment very close to the Brazier reference result M_{Braz} (Eq. (2)). It also produces an almost identical response to the 2D ovalisation analysis of Karamanos [11]. In both cases, the Brazier moment M_{Braz} is attainable only in very thin shells, so neither 2D analysis comes closer than within 2% of it. By contrast, although the 3D model follows almost the same initial nonlinear path, and thus correctly captures the fully-developed pre-buckling ovalisation response when $\Omega = 7$ or beyond as the 2D model, it only reaches a moment approximately 6% below M_{Braz} (or 49% below M_{cr}) before bifurcating onto a distinct post-buckling path.

3. Computed relationship between the buckling moment and length

The predictions of the 3D finite element simulations are presented here through a series of computed relationships between the dimensionless characteristic moment M_k/M_{cr} and the dimensionless length parameter Ω for varying yield strengths (235, 355 and 460 MPa) and a wide range of d/t ratios (from 40 to 1400). The lengths were chosen to span a wide range of qualitative behaviours, from 'medium' cylinders unaffected by ovalisation ($\Omega < 0.5$) to 'long' cylinders under full-developed ovalisation ($\Omega > 7$) and 'transitional' ones in-between. The GNA predictions were originally performed in the Rotter *et al.* [9] study and provide a valuable point of reference by denoting the buckling moment affected by ovalisation and local bifurcation buckling but not plasticity. MNA and GMNA predictions are additionally shown, where the MNA is based on small displacement theory and thus cannot model any geometrically nonlinear effects or bifurcations.

A selection of moment-curvature equilibrium paths for a selection of d/t at $\Omega = 0.5$ and 7 are shown in Fig. 4, while the full moment-length relationships are presented in Fig. 5. The curves are purposefully presented in terms of varying σ_y at constant d/t instead of $d/(t\varepsilon^2)$ to illustrate the influence of changing the yield strength on the predicted moment capacity. When the tube is short and thick, the elastic critical buckling moment M_{cr} is significantly greater than the full plastic moment M_{pl}, such that the latter will control as the limiting resistance. For short tubes ($\Omega < 0.5$), there is negligible ovalisation and thus negligible nonlinearity on the fundamental elastic path, and both MNA and GMNA predict a very similar ultimate moment M_k (Fig. 5, top-left). For very long and thick tubes susceptible to ovalisation ($\Omega > 7$), the Brazier moment M_{Braz} will also significantly exceed M_{pl}, which then also controls as the limiting resistance. Further, as the initial portion of the Brazier equilibrium path is very linear (Fig. 3), the response would have to proceed very far up this path in order to reach the nonlinear portion where ovalisation begins to noticeably degrade the pre-buckling stiffness. The response of a thick tube under cannot bending cannot achieve this, being limited by $M_{pl} < < M_{cr}$ or M_{Braz}, and thus it remains confined to a linear region of the equilibrium path that remains ovalisation-free such that MNA ≈ GMNA for all Ω (Fig. 5, top-left). However, local buckling may still cause a GMNA prediction to fall slightly beneath that of a MNA (Fig. 4, top-right).

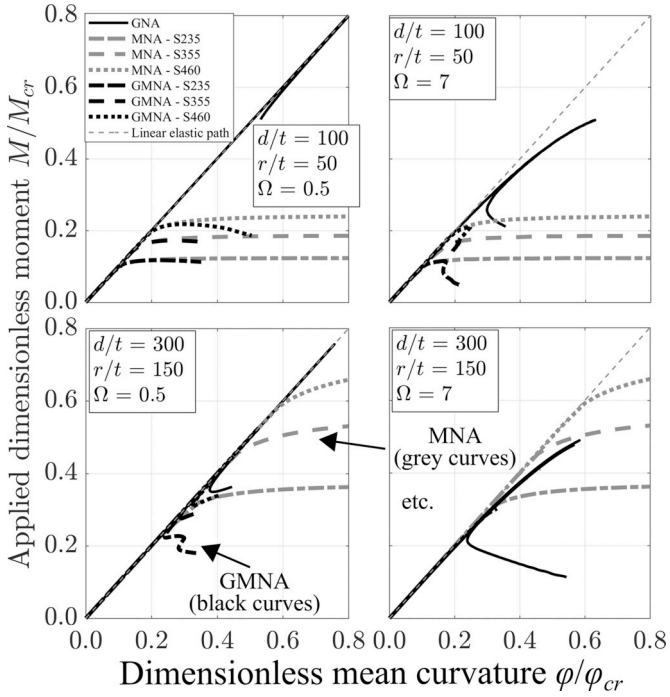

Fig. 4. Computed MNA, GNA and GMNA moment-curvature paths for three yield strengths (235, 335 and 460 MPa) and d/t or r/t ratios.

The effect of making the tube more slender by increasing the d/t ratio or the yield strength σ_y is to permit a convergence of M_{pl} to either M_{cr} or M_{Braz} such that the tube's response begins to cover an increasingly large portion of the theoretical elastic equilibrium path (Fig. 4, bottom). In the case $\Omega \to 7$, this leads to an increasing involvement of the upper nonlinear portions of the path as $M \to M_{Braz}$. Thus, as Ω, d/t and σ_y increase, Fig. 5 shows a growing divergence between MNA and GMNA, with the GMNA predictions becoming increasingly affected by pre-buckling ovalisation. The modern tendency to use increasingly higher-strength steels in circular hollow sections should be seen in this context, as their response to bending will involve a larger portion of the nonlinear fundamental elastic path at any Ω and thus risks being more affected by ovalisation than a tube of a lower grade of steel. In all cases, the theoretical GNA prediction (dotted lines in Fig. 5) acts as an upper bound to the GMNA predictions but not the MNA ones, and for very thin cylinders GNA ≈ GMNA.

4. Computed relationship between the buckling moment and cross-section slenderness

These results consider only tubulars that are long enough to exhibit the most nonlinear possible fundamental elastic path corresponding to 'fully-developed' ovalisation (i.e. Fig. 3), regardless of how far they may proceed up it before reaching a limit state. The computed relationships between M_k/M_{Braz} and $d/(t\varepsilon^2)$ for MNA and both 2D and 3D GMNA are presented in Fig. 6. The 3D GMNA system was analysed at $\Omega = 7$, while the 2D plane strain GMNA system corresponds to an 'infinitely' long tube. Although the focus is nominally on thick tubes with low $d/(t\varepsilon^2)$, the relationship is extended to very slender cylinders for completeness. In the slenderness domain widely accepted as 'stocky' ($d/(t\varepsilon^2) \leq \sim 70$), the difference between MNA and both types of GMNA analyses is almost negligible and thus the tube fails essentially by plastic collapse at a moment very close to M_{pl} with very little influence of any geometrically nonlinear effect. This is entirely consistent with the tendency observed in test results (Fig. 1). With increasing $d/(t\varepsilon^2)$, the 2D GMNA predictions approach M_{Braz} asymptotically, whereas the 3D GMNA predictions settle on a moment approximately 5% below this moment.

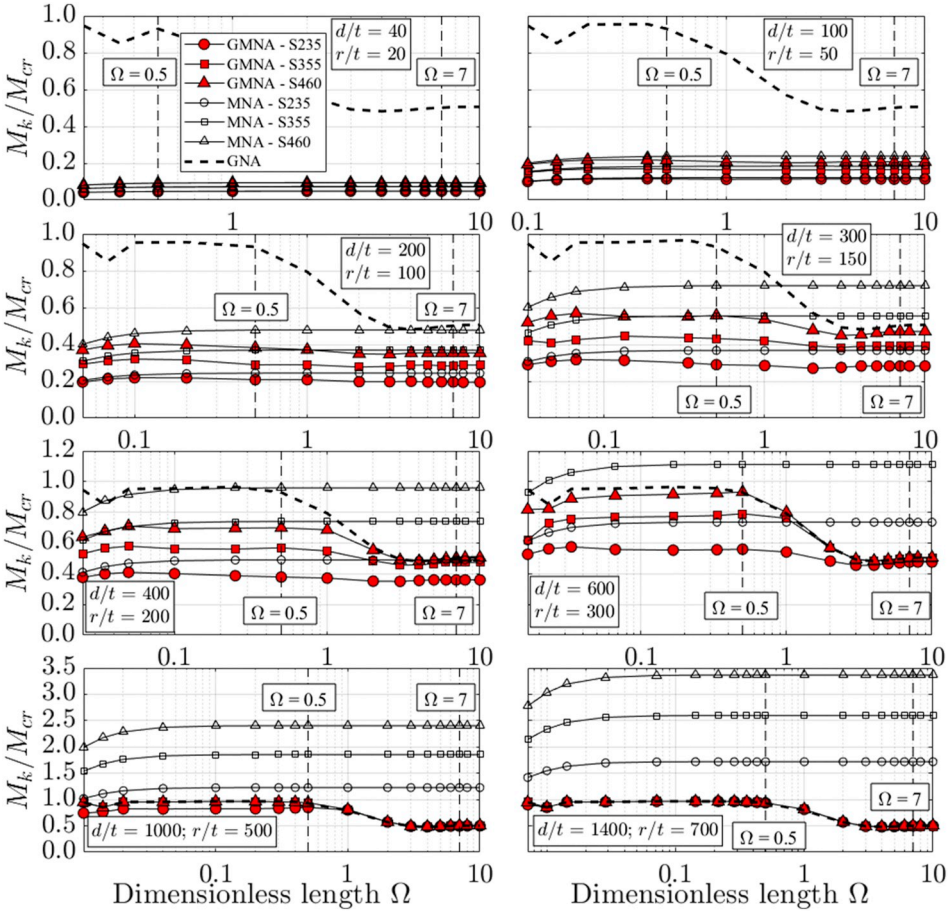

Fig. 5. Computed MNA, GNA and GMNA relationships between the dimensionless characteristic resistance M_k/M_{cr} against the dimensionless length $\Omega = L/\sqrt{(rt)}$ for three yield strengths (235, 335 and 460 MPa) and varying d/t (r/t) ratio.

The same data is presented in an alternative format in terms of M_k/M_{pl} against $d/(t\varepsilon^2)$ in Fig. 7. The GMNA predictions suggest that M_k may never quite reach M_{pl} as $d/(t\varepsilon^2) \rightarrow 0$, a consequence of no strain hardening in the assumed material law (see Fig. 1 in Sadowski *et al.* [17]. Real steels exhibit strain hardening, and thus real tubes attain M_{pl} at a finite value of $d/(t\varepsilon^2)$. The ideal elastic-rigid plastic assumptions employed here thus provides an *upper* bound on the damaging influence of ovalisation on M_k, since any strain hardening would cause an increase in M_k bringing it closer to M_{pl}. Under this conservative assumption, Fig. 7 shows that the reduction on M_k due to pre-buckling

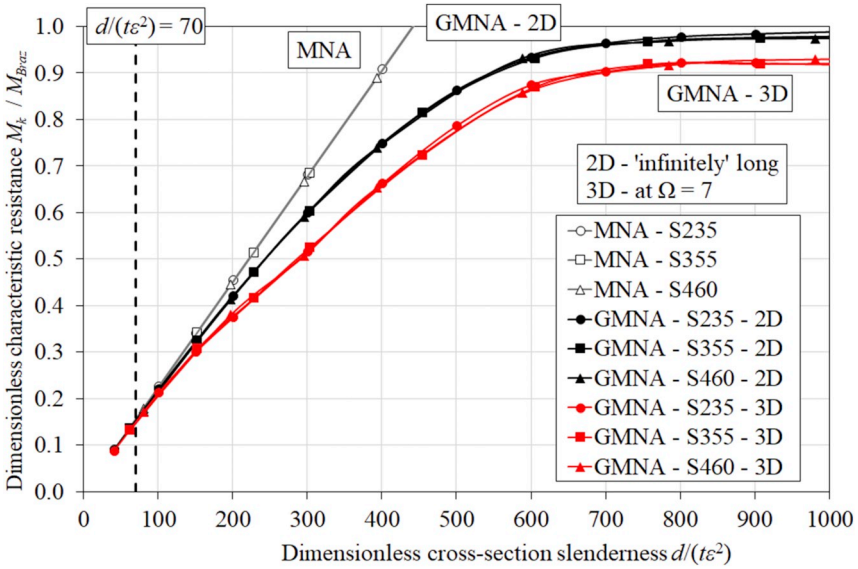

Fig. 6. Computed MNA, GNA and GMNA relationships between the dimensionless characteristic resistance M_k/M_{Braz} against the dimensionless cross-section slenderness $d/(t\varepsilon^2)$ for three yield strengths (235, 335 and 460 MPa).

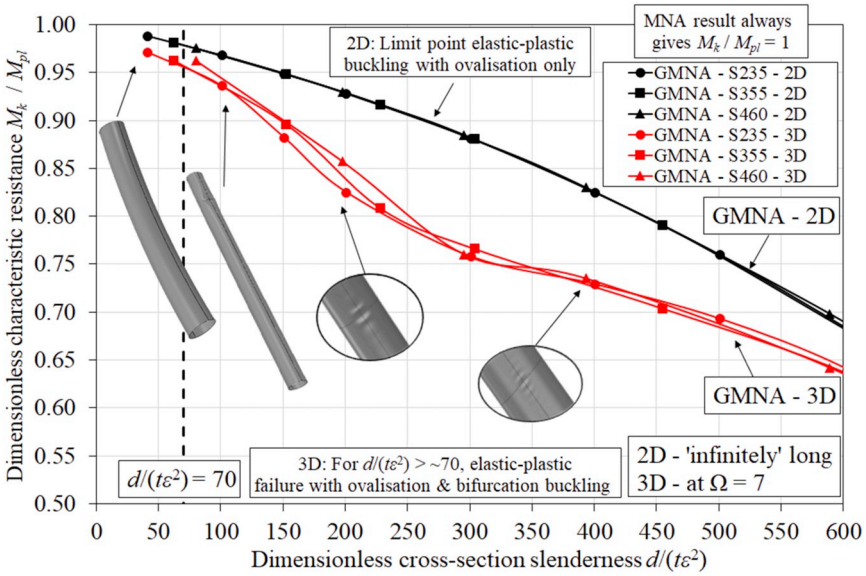

Fig. 7. Computed GNA and GMNA relationships between the dimensionless characteristic resistance M_k/M_{pl} against the dimensionless cross-section slenderness $d/(t\varepsilon^2)$ for three yield strengths (235, 335 and 460 MPa).

geometric nonlinearity is less than 5% for tubes with $d/(t\varepsilon^2)$ below 150. At large section slendernesses, however, the deleterious effect of pre-buckling geometric nonlinearity increases steadily. At $d/(t\varepsilon^2) \approx 250$ (roughly the upper limit of test specimens in the past; Fig. 1), the reduction in M_k from M_{pl} due to geometric nonlinearity is approximately 20%, although only 10% is attributable to ovalisation with the remainder due to bifurcation buckling on the compressed side.

The authors stress that these predictions relate to the very conservative condition of fully-developed ovalisation ($\Omega > 7$) under uniform bending. Many of the test results conducted in the past (Fig. 1) are significantly shorter than this, thus the influence of ovalisation on the moment capacity may be expected to be even *milder*. Additionally, conditions of truly uniform bending are rare and the effect of a moment gradient is to mollify the nonlinearity of the fundamental path due to ovalisation [18], reducing its detrimental effect on thick tubes yet further.

5. Conclusions

This paper has presented a detailed computational investigation that attempted to quantify the extent to which ovalisation may be expected to decrease elastic-plastic moment resistance of tubes under bending. This was achieved by a comprehensive parametric study of idealised perfect tubes with an elastic-plastic material law and uniform bending through a selection of different types of computational analyses. It is hoped that this study will provide guidance to designers of test programmes and drafters of structural Standards on the potential for ovalisation to affect the plastic resistance behaviour of thick tubulars and hollow sections under bending loads.

It is found that even under the most conservative conditions of no strain hardening, no pressurisation, uniform bending and 'infinite' length, ovalisation is likely to be responsible for only a negligible reduction in the reference full plastic moment capacity in a thick tubular. For thick tubes with slenderness up to $d/(t\varepsilon^2)$ up to ~100, the reduction is less than 5%. Any *significant* negative discrepancies of tested thick tubulars with the full plastic moment in this slenderness domain are therefore likely attributable to other reasons, most likely deep imperfections in the tube or errors in the testing process. The influence of geometric imperfections is currently being investigated by the authors and will be quantified in an upcoming study.

Acknowledgements

This work was partly funded by the UK Engineering and Physical Sciences Research Council (EPSRC) with grant contract EP/N024060/1.

Appendix A. Supplementary data

Supplementary data related to this article can be found at https://doi.org/10.1016/j.ijpvp.2018.05.004.

References

[1] R.M. Korol, Critical buckling strains of round tubes in flexure, Int J Mech Sci 22 (1979) 719–730.
[2] M.J. Stephens, G.L. Kulak, C.J. Montgomery, Local buckling of thin walled tubular steel members, SE Report N. 103 University of Alberta, 1982.
[3] A.M. Gresnigt, R.J. van Foeken, Local buckling of UOE and seamless steel pipes, Proc. 11th int. Offshort & polar eng. Conference, 2001, pp. 131–142 17–22 June, Stavanger, Norway.
[4] RFCS Combitube, Bending resistance of steel tubes in combiwalls – final report, (2014) Research Fund for Coal and Steel, Grant Agreement RFSR-CT-2011–20100034.
[5] D.J. Peters, A.J. Sadowski, J.M. Rotter, A. Taras, Calibration of Eurocode design models of thin-walled cylinder under bending with full scale tests, Proc. Eurosteel 2017, september 13-15, 2017 Copenhagen, Denmark.
[6] C. Buchanan, L. Gardner, A. Liew, The continuous strength method for the design of circular hollow sections, J Constr Steel Res 118 (2016) 207–216.
[7] S.B. Batdorf, A simplified method of elastic-stability analysis for thin cylindrical shells. II – modified equilibrium equation, NACA Technical Note 1342, Washington D.C (1947).
[8] C.R. Calladine, Theory of shell structures, Cambridge University Press, 1983.
[9] J.M. Rotter, A.J. Sadowski, L. Chen, Nonlinear stability of thin elastic cylinders of different length under global bending, Int J Solid Struct 51 (2014) 2826–2839.
[10] L.G. Brazier, On the flexure of thin cylindrical shells and other 'thin' sections, Proc. Royal Society Series A 116 (1927) 104–114.
[11] S. Karamanos, Bending instabilities of elastic tubes, Int J Solid Struct 39 (2002) 2059–2085.
[12] A.M. Gresnigt, S. Karamanos, Local buckling and deformation capacity of tubes in steel structures, in: J.F. Chen, J.Y. Ooi, J.G. Teng (Eds.), Structures and granular solids – from scientific principles to engineering applications, CRC Press, 2008, pp. 199–217.
[13] Dassault Systèmes, ABAQUS 2017, Commercial Finite Element Software, 2017.
[14] EN 1993-1-6, Eurocode 3: design of steel structures. Part 1-6: strength and stability of shell structures, Comité Européen de Normalisation, Brussels, 2007.
[15] A.J. Sadowski, J.M. Rotter, Solid or shell finite elements to model thick cylindrical tubes and shells under global bending, Int J Mech Sci 74 (2013) 143–153.
[16] Z. Xu, L. Gardner, A.J. Sadowski, Nonlinear stability of elastic elliptical cylindrical shells under uniform bending, Int J Mech Sci 128–129 (2017) 593–606.
[17] A.J. Sadowski, J.M. Rotter, T. Reinke, T. Ummenhofer, Statistical analysis of the material properties of selected structural carbon steels, Struct Saf 53 (2015) 26–35.
[18] J. Wang, A.J. Sadowski, Elastic imperfect cantilever cylinders of varying length, Int J Mech Sci 140 (2018) 200–210.